Jones, T. A., & Thirup, S. (1986) *EMBO J. 5*, 819-822.
Ju, G., Campen, C. A., Benjamin, W. R., Labriola-Tompkins, E., Karas, E., Plocinski, J., Biondi, D., Kaffka, K., Kilian, P. L., Eisenberg, S. P., & Evans, R. J. (1991) *Proc. Natl. Acad. Sci. U.S.A.* (in press).
Kamogashira, T., Sakaguchi, M., Ohmoto, Y., Mizuno, K., Shimizu, R., Nagamura, K., Nakai, S., Masui, Y., & Hirai, Y. (1988) *J. Biochem. (Tokyo) 104*, 837-840.
Kay, L. E., & Bax, A. (1989) *J. Magn. Reson. 86*, 110-126.
Kay, L. E., Clore, G. M., Bax, A., & Gronenborn, A. M. (1990) *Science 249*, 411-414.
Kraulis, P. J., Clore, G. M., Nilges, M., Jones, T. A., Petterson, G., Knowles, J., & Gronenborn, A. M. (1989) *Biochemistry 28*, 7241-7257.
MacDonald, H. R., Wingfield, P. T., Schmeissner, U., Shaw, A., Clore, G. M., & Gronenborn, A. M. (1986) *FEBS Lett. 209*, 295-298.
Marion, D., Kay, L. E., Sparks, S. W., Torchia, D. A., & Bax, A. (1989a) *J. Am. Chem. Soc. 111*, 1515-1517.
Marion, D., Driscoll, P. C., Kay, L. E., Wingfield, P. T., Bax, A., Gronenborn, A. M., & Clore, G. M. (1989b) *Biochemistry 28*, 6150-6156.
Mosley, B., Dower, S. K., Gillis, S., & Cosman, D. (1987) *Proc. Natl. Acad. Sci. U.S.A. 84*, 4572-4576.
Mueller, L. (1987) *J. Magn. Reson. 72*, 191-196.
Nilges, M., Clore, G. M., & Gronenborn, A. M. (1988) *FEBS Lett. 229*, 317-324.
Nilges, M., Clore, G. M., & Gronenborn, A. M. (1990) *Biopolymers 29*, 813-822.
Priestle, J. P., Schär, H.-P., & Grütter, M. (1989) *Proc. Natl. Acad. Sci. U.S.A. 86*, 9667-9671.
Qian, Y. Q., Billetter, M., Otting, G., Müller, M., Gehring, W. J., & Wüthrich, K. (1989) *Cell 59*, 573-580.
Shaka, A. J., Lee, C. J., & Pines, A. (1988) *J. Magn. Reson. 77*, 274-293.
Sims, J. E., & Dover, S. K. (1990) in *The Year of Immunology 1989-1990* (Cruse, J. M., & Lewis, R. E., Eds.) Vol. 6, pp 112-126, Karger, Basel.
Wingfield, P. T., Payton, M., Tavernier, J., Barnes, M., Shaw, A., Rose, K., Simona, M. G., Demaczuk, S., Williamson, K., & Dayer, J.-M. (1986) *Eur. J. Biochem. 160*, 491-497.
Wingfield, P. T., Graber, P., Movva, N. R., Clore, G. M., Gronenborn, A. M., & MacDonald, H. R. (1987) *FEBS Lett. 215*, 160-164.
Wingfield, P. T., Graber, P., Shaw, A. R., Gronenborn, A. M., Clore, G. M., & MacDonald, H. R. (1989) *Eur. J. Biochem. 179*, 565-571.
Wüthrich, K., Billetter, M., & Braun, W. (1983) *J. Mol. Biol. 169*, 949-961.
Zuiderweg, E. R. P., & Fesik, S. W. (1989) *Biochemistry 28*, 2387-2391.
Zuiderweg, E. R. P., McIntosh, L. P., Dahlquist, F. W., & Fesik, S. W. (1990) *J. Magn. Reson. 86*, 210-216.

Articles

X-ray Absorption Fine Structure Investigation of the Zinc Transition Metal Binding Site of Zn Concanavalin A in Solution and in the Crystal†

S.-L. Lin,‡ E. A. Stern,*,‡ A. J. Kalb (Gilboa),§ and Y. Zhang‡

Department of Physics FM-15, University of Washington, Seattle, Washington 98195, and Department of Biophysics, Weizmann Institute of Science, Rehovoth, Israel

Received September 6, 1990; Revised Manuscript Received December 4, 1990

ABSTRACT: We report details on measurements by the X-ray absorption fine structure (XAFS) technique of the conformational changes around the transition metal binding site (S1) of the protein concanavalin A induced by crystallization when that site is occupied by Zn. A change from hexa- to tetracoordination occurs at the S1 site on crystallization when the calcium-binding site (S2) is occupied by a calcium atom. When the S2 site is unoccupied, the Zn is pentacoordinated both in solution and in the crystal. The average distance to the coordination shell increases with coordination number as expected. Conformational changes are detected up to 4.5 Å from the Zn, the limit of sensitivity of the XAFS technique. When the Zn is hexacoordinated, the ligands around the Zn, as determined by XAFS, are consistent with the crystal structure determination results of five oxygens and one nitrogen. The atom that is released when the coordination decreases to five is an oxygen atom, and, in addition, the nitrogen is released in the tetracoordinated Zn. Thus, when S2 is emptied, the protein gains a ligand about the Zn site in the crystal and loses one in solution. These results provide direct evidence that the protein conformation can be altered by the intermolecular forces of crystallization.

The foundation of our understanding of the mechanism of the functioning of proteins is knowledge of their structure, and almost all of the information on protein structure has come from X-ray diffraction studies on the crystalline state. Recently we reported structural differences in the protein concanavalin A between its solution and crystal forms (Lin et al., 1990). This finding raises once more the question of how generally one can relate the crystalline structure of proteins to their behavior in solution. Although our recent XAFS work is the first that *directly* compared the structure of a protein in a crystal and in solution by the same technique, there have been other indications of structural differences in proteins

† This work was funded by NSF under Grant DMB-8613948.
‡ University of Washington.
§ Weizmann Institute of Science.

0006-2960/91/0430-2323$02.50/0

caused by the intermolecular interactions imposed by the crystal structure. In all these other cases, the differences have been suggestive or qualitative and not definitive or quantitative because either the techniques only indirectly probed the structure or the changes were found by a different technique for each state of the protein. Differences have been found (Johansen & Vallee, 1975) in the color of carboxypeptidase A modified with diazotized arsanilic acid. In solution the modified protein has a red color, but in the crystal the modified protein has either a yellow (Johansen & Vallee, 1975) or a red color (Quiocho et al., 1971) depending on whether it is the γ or α isozyme, respectively. The native isozymes both crystallize in a monoclinic space group but with somewhat different unit cell parameters. Only the structure of the α isozyme has been determined by X-ray crystallography (Reeke et al., 1967; Quiocho et al., 1971); that of the γ form is still unknown. It has been suggested (Johansen & Vallee, 1975) that the different color of the two crystal forms is due to different complexing between the Zn cofactor and arsanilazotyrosine-248. Whatever are the actual structural differences that cause the color differences, the important aspect for our consideration is that there is a structural difference induced by crystallization forces between the two different crystals that disappears when they dissolve. Resonance Raman studies of metmyoglobin (Sage et al., 1989) find differing scattering intensities of the 345-cm^{-1} mode in solution and crystalline forms, which indicates a structural perturbation of the heme upon crystallization. NMR studies of polypeptides in solution [Wüthrich (1989) and references cited therein: Kline et al., 1986; Pflugrath et al., 1986; Wagner et al., 1986; Clore et al., 1987] have found differences with the crystal structures, as, for example, in the case of the hormone glucagon and the metal-rich protein metallothionein (Braun et al., 1983; Schultze et al., 1988).

X-ray absorption fine structure spectroscopy (XAFS) has advantages for this kind of investigation: it applies to solution and solid phases equally well with high precision, and the spectrum is interpretable directly in structural terms (Stern & Heald, 1983). XAFS determines the structure locally around specific atoms, which can be chosen by tuning the X-rays to the appropriate absorption edge. For macromolecules, a practical usage of XAFS is to examine heavy atoms present in the molecules. Metalloproteins are a natural object of this technique. These proteins have a small number of metal atoms as an integrated part of the molecule, in addition to the lighter atoms that compose the rest of the protein. XAFS is capable of solving the metal-site structure in a range of a few angstroms around the metal atom. Typically, it is possible to determine the number of atoms surrounding the metal atom, their types, and their average distances from the metal atom, as well as the disorder about the average. There is no fundamental difference in the measurement between a protein solution and the crystal beyond those of normal sample preparation. A comparison of the spectra collected from these protein samples constitutes a straightforward comparison between the structures of the protein in different physical states.

Concanavalin A, a saccharide-binding protein from jack bean (*Canavalia ensiformis*), has two distinct metal sites. One of them, S1, is a transition metal site, and the other, S2, can contain either a Ca or a Cd atom. Depletion of metal from S2 does not denature the protein but destroys its saccharide-binding site (Yariv et al., 1967; Kalb & Levitzki, 1968). Investigations on a concanavalin A sample with Zn in S1 and Ca in S2 have been reported earlier (Kalb et al., 1979; Lin et al., 1990). We found that in solution the Zn atom had one more ligand and a longer average ligand bond length than in the crystal. Also, the disorder of the Zn coordination shell increased normally with temperature in solution, whereas it showed a null change in the crystal. We suggested that these differences were the results of the intermolecular interactions in the crystalline lattice on the protein molecules. The intermolecular interactions produce conformational changes in the protein, causing modification at the Zn site. On cooling we find that the crystalline restrictions subject the Zn site to a tensile stress, which causes a weakening of the ligand bonds and the anomalous temperature dependence of the vibrational amplitude. In this article we give a more detailed analysis (under Analysis and Results) of the differences at the S1 site of concanavalin A between the crystal and solution, which suggests that the zinc in the crystal is tetracoordinated, not pentacoordinated, indicating an even larger change on crystallization. In contrast, when the S2 site has its Ca atom removed, there is no change found around the Zn site on crystallization.

Materials and Methods

Concanavalin A was prepared from jack bean meal by the method of Sumner and Howell (1936). Solutions were prepared by removal of the naturally occurring metals by acid treatment and addition at pH 5.2 (0.05 M sodium acetate) of Zn salt, and of Ca salts as required (Shoham et al., 1973). The solutions were 1 M in NaCl in order to achieve a protein concentration greater than 1 mM. The free Zn concentration in solution was no more than 5% of the protein concentration (Shoham et al., 1973). Polycrystalline slurries were prepared as described for *I*222 crystals of concanavalin A prepared for X-ray diffraction study by equilibration of the above solutions against 0.1 M $NaNO_3$ at pH 6.5 (Greer et al., 1970). For temperature-dependence study, 40% (by weight) galactose (Sigma grade crystalline, Sigma, St. Louis, MO) was added to the solutions and 50% 2-methyl-2,4-pentanediol (MPD) to the polycrystalline slurries to inhibit formation of ice crystals at low temperatures. For cryogenic experiments, ice suppression was attained by quenching the room-temperature solution into liquid nitrogen. Besides minimizing the possibility of damage to the protein, ice inhibition also eliminated a noise background of Bragg peaks in the XAFS data. Protein samples without cryoprotectant were also measured at room temperature to examine the effects of the cryoprotectants.

XAFS experiments were performed at the NSLS X-11 beam line. Harmonic rejection was accomplished by about a 20% detuning of the Si(111) double-crystal monochromator. The incident intensity I_0 was monitored by a semitransparent gas ionization chamber. The protein samples were measured at the Zn K-edge in a fluorescence mode by using a Soller-slit filter arrangement (Stern & Heald, 1983) with an ion chamber detector filled with Kr gas. Standard compounds (listed below) were prepared as powders and measured in a transmission mode by using a gas ionization chamber to detect the transmitted intensity. The powder used in all cases was fine enough so that thickness effects were negligible (Lu & Stern, 1983). Standards and protein samples were measured at 80 and 300 K under the same beam-line conditions to minimize systematic differences due to varying energy resolution, etc. Low temperatures were maintained with an Air Products Displex refrigerator during the measurements. Measurements of proteins at 300 K were repeated before and after cryotemperature measurements. No significant difference was found between the two sets of 300 K data, indicating no damage occurred around the Zn site on cooling or on exposure to X-rays. The small percentage of Zn atoms not incorporated in the proteins

in solution (<5%) will give an error to the protein structure that is within our other uncertainties. The polycrystals that composed the slurries were fine enough so that hundreds of them were illuminated by the X-ray beam, assuring no appreciable preferred orientation effects.

Theory

We give a brief description of the XAFS theory in the following. For more complete presentations and discussions, readers are referred to Stern and Heald (1983). In condensed matter the photoelectron excited from an atomic core state by X-ray absorption is subject to backscattering from surrounding atoms. The final photoexcited state is an interference of the outgoing and backscattered parts of the photoelectron. The interference varies with the momentum of the photoelectron and gives rise to a modulation, the XAFS spectrum, in the X-ray absorption coefficient of the sample. XAFS can be expressed by the formula

$$\chi(k) = \sum_j \frac{f_j(k)}{kR_j^2} e^{-2k^2\sigma_j^2} \sin [2kR_j + \delta_j(k)] \qquad (1)$$

where $\chi(k)$ is the XAFS, k is the wavenumber of the photoelectron, R_j is the distance of the excited atom to the jth backscattering atom with variation σ_j, $f_j(k)$ is the magnitude of the effective scattering amplitude of the jth atom, and $\delta_j(k)$ is a phase depending on both the central and the backscattering atoms. Summation is carried over all the backscattering atoms.

$\chi(k)$ is obtained from the X-ray absorption spectrum of the sample near an absorption edge, $\mu(k)$, by subtracting $\mu_0(k)$, a smoothly varying portion past the edge that physically corresponds to the absorption of an isolated atom, and normalizing against the step size of the absorption edge, $\Delta\mu_0$:

$$\chi(k) = \frac{\mu(k) - \mu_0(k)}{\Delta\mu_0} \qquad (2)$$

The photoelectron wavenumber k is given in reciprocal angstroms by $k^2 = 0.263(E - E_0)$, where E is the X-ray energy and E_0 is the core binding energy, both in electron volts. In our case E_0 was set at the point halfway up the edge step. $\mu(k)$ can be measured either in a transmission mode or in a fluorescence mode, depending on which gives the optimum signal-to-noise ratio. In the transmission mode μ is calculated by Beer's law:

$$\mu x = \log I_0/I \qquad (3)$$

where I_0 and I are the photon fluxes before and after the sample, respectively, and x is the sample thickness. In the fluorescence mode for dilute samples, μ can be obtained from the fluorescence signal I_f by

$$\mu = I_f/cI_0 \qquad (4)$$

where c is related to the concentration of the atoms of interest and the detection efficiency of fluorescent X-rays emitted after the atomic excitation. Dividing the edge step as per eq 2, the coefficients x in eq 3 or c in eq 4 cancel.

In normalizing I by I_0, somewhat different results are obtained for the transmission and fluorescence measurements. Since I_0 is monitored by a semitransparent gas ionization chamber, its signal is proportional to the fraction of I_0 being adsorbed in the gas. This fraction decreases as the energy of the X-ray in I_0 increases. In transmission this energy dependence just adds to the smooth background, which is eliminated in the analysis. However, in fluorescence this energy dependence remains in μ, increasing its value with energy. When comparing the sample measured by fluorescence with standards measured by transmission, a correction has to be applied to compensate for this effect. In our case we used tabulated X-ray absorbance of the I_0 chamber gas (McMaster et al., 1969) to correct for this effect. For Zn in concanavalin A it is equivalent to adding a disorder term of 0.001 Å^2 to the fluorescence result.

Equation 1 presents k and R as a pair of Fourier variables. A Fourier transform qualitatively separates the scattering of the surrounding atoms along R. Before Fourier transformation, a weighting function of k is applied to χ to enhance the radial separation in R-space. The first neighbor coordination shell can be separated in this manner. More distant shells are normally not separated and are further complicated by multiple scattering effects. For this reason we give a quantitative analysis for only the first neighbors. The first shell can be isolated in R-space and then inverse-transformed back to k-space to obtain a single-shell expression for $\chi(k)$ with the sum over only the first neighbors.

We treat the single-shell XAFS spectrum in two different ways. One of them is the *log ratio* method. In this method the atoms in the shell are assumed to be the same so that both $f(k)$ and $\delta(k)$ are independent of j. Their only difference is in R, whose effect can either be incorporated in an increased mean squared disorder σ^2 and other cumulants (Stern & Heald, 1983) or be removed explicitly by a structure factor

$$S(k) = \sum_j \frac{1}{R_j^2} \exp(i2kR_j) \qquad (5)$$

if all R's are precisely known. If two species have a matched central atom and a shell composed of the same type of atoms, the ln ratio method is highly convenient in comparing their shell structures, especially when they are not too dissimilar and the lowest cumulants can be used.

$$\log \frac{A_1}{A_2} = \log \left(\frac{N_1}{N_2} \frac{R_2^2}{R_1^2} \right) - 2k^2\Delta\sigma^2 \qquad (6)$$

$$\phi_1 - \phi_2 = 2k\Delta R \qquad (7)$$

where A_1 and A_2 are the amplitudes and ϕ_1 and ϕ_2 are the phases of the two spectra, respectively, N_1 and N_2 are the numbers of atoms in the shell, R_1 and R_2 are the average distances, ΔR is their difference, and $\Delta\sigma^2$ is the difference of the mean square disorder. N_1/N_2, ΔR, and $\Delta\sigma^2$ describe the structural differences of the two species. The strict atom-type match requirement of the method may be relaxed somewhat to allow a small number of heterogeneous atoms in the shell. It will produce additional uncertainty, which should be considered properly in the analysis.

The other approach is a fitting method. This method reconstructs sample spectra from the XAFS spectra of several model compounds, combined linearly as described by eq 1. The model compounds have the same central atom as the sample, surrounded by the same atoms that are presumed to be present in the sample. A least-squares fitting algorithm is used to determine the number of surrounding atoms of various types, their distances to the central atom, and the disorder around the distances. The goodness of the fitting is assessed by the criterion set by Zhang et al. (1988) and Lytle et al. (1989), with a normalized χ^2 function described by Bevington (1969) as

$$\chi_\nu^2 = \frac{1}{\nu} \sum_j \frac{(\chi^i - \chi_f^i)^2}{(\sigma^i)^2} \qquad (8)$$

where $\nu = N_1 - P$.

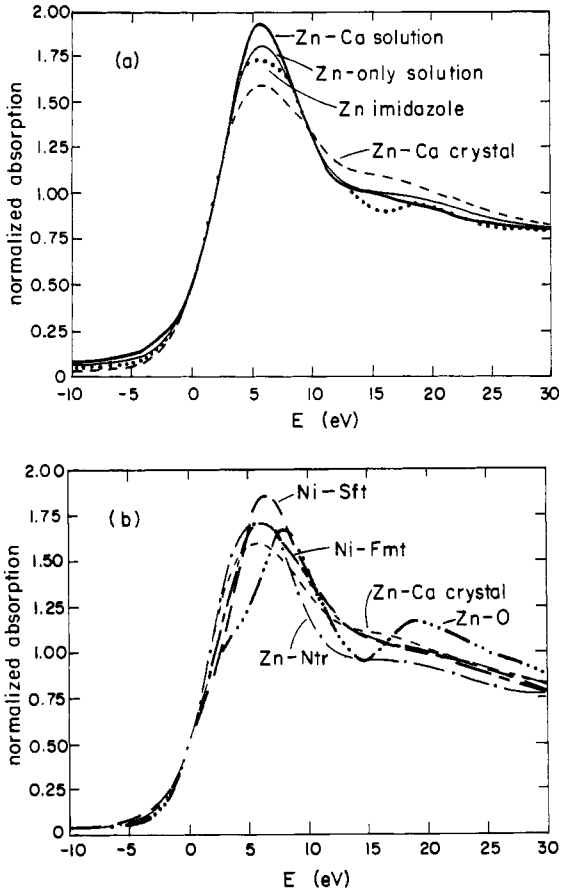

FIGURE 1: (a) Room-temperature near-edge spectra of Zn-Ca concanavalin A solution (—, heavy), Zn-Ca concanavalin A crystal (dash (---), Zn-only concanavalin A solution (—, light) and Zn-imidazole (···). (b) Room-temperature near-edge spectra of Zn-Ca concanavalin A crystal (dash (---) and the standards: Zn-Ntr (—·—), Ni-Sft (— —), Ni-Fmt (— · —), and Zn-O (— ··· —).

Here χ^i is the experimental value at the independent point i and χ_f^i is the corresponding fit. The experimental uncertainty at i is σ^i. The normalization by the degrees of freedom ν accounts for the number of independent points N_I that the data contain and the decrease in the independence of the number of data points by the introduction of P parameters in the fitting model. This method gives an objective way to assess whether a fit is acceptable or not by the requirement that $\chi^2 \lesssim 1$. In essence, when χ^2 is of the order of 1, the fit is within about a standard deviation of the experimental uncertainties.

The number of independent points is given by

$$N_I = (2/\pi)\Delta k \Delta R + 1 \qquad (9)$$

where Δk is the range of k with usable signal and ΔR is the range in R-space of the window isolating the first shell. It should be noted that the number of independent points is not determined by the number of points measured in the XAFS spectrum but is typically much smaller. In our case ΔR = 1.1 Å and Δk = 8 giving a value of $N \approx 7$. The reason that the number of independent points is limited in k-space is because the frequency content of the first shell is limited by its finite width in R-space. For example, if a sine wave has only a single frequency, the amplitude of the wave as a function of time is constant and knowledge of the amplitude at one time determines its value for all time; i.e., there is only one independent value or point for the amplitude. However, if a wave has a finite range of frequencies $\Delta\omega$ associated with it, then the amplitude of the wave can vary with time but the time interval δt required before the amplitude has a value uncorrelated to the initial value is $\delta t \approx \pi/\Delta\omega$. Thus there is a finite

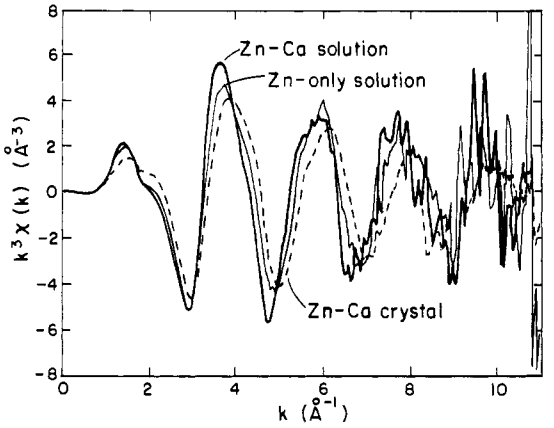

FIGURE 2: Room-temperature XAFS $k^3\chi(k)$ for the protein samples: Zn-Ca concanavalin A solution (—, heavy), Zn-Ca concanavalin A crystal (---), and Zn-only concanavalin A solution (—, light).

spacing in t between independent points and the number of independent points is given by dividing the total range of t by this spacing (Lee et al., 1981) and adding 1. In our case, the Fourier pairs are $2k$ and R instead of ω and t, leading to eq 1. The one is added on the right because there is one more point than spaces.

A key element of the fitting routine is the uncertainties that enter into σ_i^2 of eq 8. There are three contributing factors to the uncertainties. These are measurement errors, uncertainties due to lack of transferability between the standards and the unknown, and uncertainties introduced by analysis. The proteins are dilute enough that the measurement errors are typically dominated by the shot noise of the finite number of fluorescence photons detected. This noise is determined by the fluctuations between independent scans of the spectra. The analysis uncertainties are determined by varying in the analyses the background subtraction and window functions used for isolating the first shell in R-space. As much as possible the protein and standard are treated similarly in their variations, and in all cases the variations are chosen so that they have reasonable windows and backgrounds. The best window is uncertain because the XAFS due to the first neighbors is not entirely isolated in R-space but has wings that overlap other shells of atoms and vice versa. Also the background is not known exactly but is subtracted off by assuming that it is varying more slowly and smoothly then the XAFS. This is done by a spline fit with several nodes but there is some arbitrariness in the process, such as how many and where the nodes are placed.

The transferability uncertainties are an attempt to account for the fact that the chemical and charge environment around the center atom is not the same for the protein as for the standards. These differences cause some variation in the backscattering for a given atom. A good standard is one that has the same center atom with similar electronic charge around it as the unknown. However, in general, the ligands of the standard are different from those of the unknown because, by necessity, the standard has only one type of atom in its ligands while the unknown, generally, will have a mixture of atoms. In our case we estimate the uncertainty in the transferability of backscattering amplitude by comparing the backscattering amplitude of different standards, all of which are good standards, to that of the unknown. Such an estimate is admittedly crude, but it is important to include such an estimate since it is a significant contribution.

To assess whether a standard is a good one we compare its near-edge spectrum with that of the protein. Figure 1 shows the near-edge spectra of the three forms of the protein that we have investigated here and the three oxygen standards plus

Table I: Structural Changes in Zn Concanavalin A Proteins As Determined by the Log Ratio Method[a]

	N_1/N_2	$\Delta\sigma^2$ (Å^2 × 10^{-3})	ΔR (Å)
soln vs cryst, 300 K	1.36 (10)	1.6 (7)	0.078 (6)
soln vs cryst, 80 K	1.30 (10)	−5.2 (7)	0.072 (6)
soln, 300 vs 80 K	0.93 (5)	5.8 (5)	0.002 (6)
cryst, 300 vs 80 K	0.96 (5)	−1.0 (5)	−0.004 (6)
soln, w vs w/o cryop	1.00 (5)	2.3 (5)	0.005 (6)
cryst, w vs w/o cryop	0.97 (5)	0.2 (5)	0.004 (6)
soln, w vs w/o Ca	1.26 (10)	1.5 (7)	0.033 (6)
cryst, w vs w/o Ca	0.81 (6)	0.8 (6)	−0.045 (20)
cryst, w vs soln w/o Ca	0.91 (10)	0.8 (7)	−0.039 (6)

[a] $\Delta\sigma^2$ is the difference in the mean squared disorder, ΔR is the difference in average bond length, and N_1/N_2 is the ratio of the coordination numbers. Soln and cryst refer to concanavalin A samples, and cryop refers to cryoprotectant, which is MPD for the crystal and galactose for solution. The samples are bound with Ca if not specified. The last five comparisons were taken at room temperature. The cryst w vs w/o Ca comparison was made earlier (Kalb et al., 1979).

ZnO. All of the samples have been normalized to 1 at the point where the extrapolated background intersects the edge. They have also been aligned on the zero of energy at the normalized absorption value of 0.5. Although two of the standards have Ni center atoms instead of the Zn atoms of the proteins, they all have six oxygen ligands and Ni and Zn are close enough in atomic number that the shapes of the near-edge spectra reflect faithfully their relative charge distributions. It is the variation in charge distribution that is the cause of any lack of transferability. It is noted that variation in the near-edge spectra between the standards nickel sulfate dihydrate (Ni-Sft) (Wyckoff, 1962), nickel formate dihydrate (Ni-Fmt) (Von Krogmann & Mattes, 1963), and zinc hexaaquo dinitrate (Zn-Ntr) (Ferrari et al., 1967) is in the same range as the differences between the three forms of the protein and their differences with Zn-Ntr, the primary standard for the oxygen backscatterer. Thus the variation of XAFS amplitude between Ni-Sft, Ni-Fmt, and Zn-Ntr is used as a measure of the transferability uncertainties. The three types of uncertainties are added together in quadrature.

The uncertainties in the parameters determined from the fitting routine were estimated by fixing one parameter off its best value an amount such that when the other parameters are varied to obtain a minimum, the value of χ^2_ν is increased by 1 from its minimum. In this case the change in the parameter increases the deviation between fit and data by about one standard error. This is a conservative estimate of the uncertainty in the parameters if there is a correlation between parameters. It determines the maximum uncertainty in a given parameter for all values of the other correlated parameters.

Analysis and Results

(*a*) *First Coordination Shell.* We have recently reported a comparison of the XAFS of crystal and solution and of the temperature dependence about the first coordination shell of Zn in concanavalin A in Zn in S1 and Ca in S2 (Lin et al., 1990). The $k^3\chi(k)$ for solution and the crystal at room temperature are shown in Figure 2. Table I lists the results obtained by a log ratio analysis. Presented are the coordination number ratio, bond length change, and difference in disorder between the protein solution and the crystal and between room temperature and cryogenic temperature. In brief, we found that in the solution the Zn has a hexacoordinated ligand shell whose disorder decreased normally with cooling. In contrast, in the crystal the Zn has a smaller coordination number, which we interpreted to be five. The ligand bonds are shorter than in solution by about 0.08 Å, and the disorder showed a null dependence on cooling. Note that the ratio of the coordination number of the solution to the crystal is about 1.36 (10), while

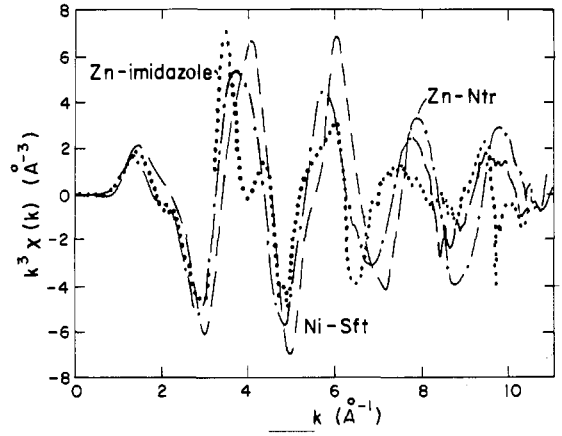

FIGURE 3: Room-temperature XAFS $k^3\chi(k)$ of the standards: Zn-Ntr (—·—), Ni-Sft (— —), and Zn-imidazole (···).

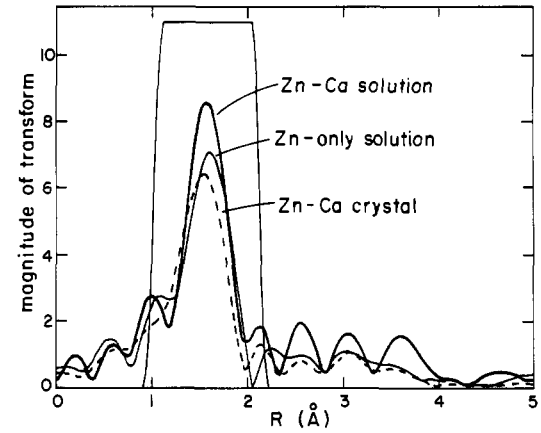

FIGURE 4: Fourier transform magnitude of the room temperature $k^3\chi(k)$ of Zn-Ca concanavalin A solution (—, heavy), Zn-Ca concanavalin A crystal (- - -), and Zn-only concanavalin A solution (—, light). Also shown is the filtering window for Zn-Ca concanavalin A solution.

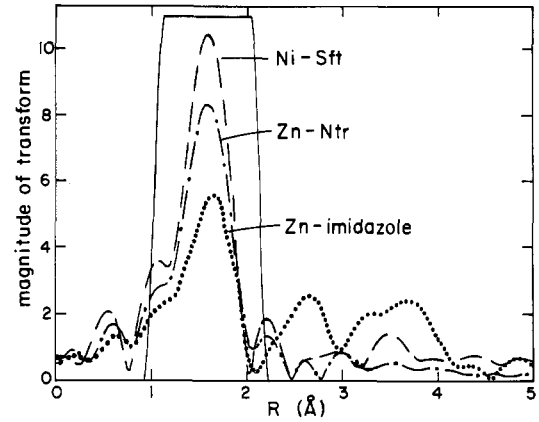

FIGURE 5: Fourier transform magnitude of the room-temperature $k^3\chi(k)$ of the standards: Zn-Ntr (—·—), Ni-Sft (— —), and Zn-imidazole (···). Also shown is the filtering window for Zn-Ntr.

pentacoordinated zinc in the crystal should ideally have a ratio of 1.20. The actual ratio is between the penta- and tetracoordinated values.

The log ratio method assumes that the ligand atoms in both the unknown and the standard are the same. This assumption is valid for the temperature dependence of the protein since the same sample is compared at different temperatures. However, for the comparison between the protein and a standard, the crystal structure of the protein indicates that there is a nitrogen ligand in addition to five oxygens (Hardman & Ainsworth, 1972; Edelman et al., 1972; Becker et al., 1975; Hardman et al., 1982). Since the standards that we employ

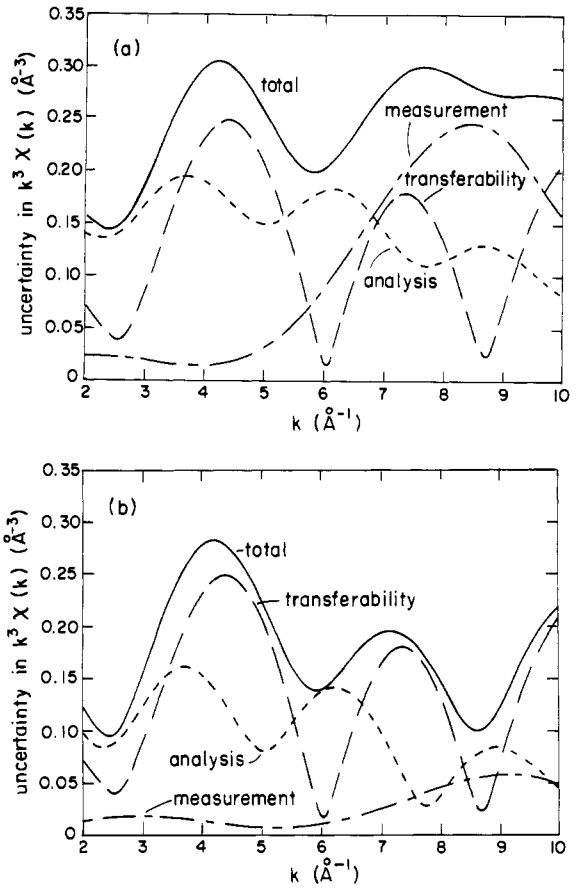

FIGURE 6: Uncertainties for fitting (a) Zn-Ca concanavalin A solution and (b) Zn-Ca concanavalin A crystal.

have all oxygen or all nitrogen ligands, the log ratio method will give some errors. However, since the difference in backscattering between nitrogen and oxygen is small and there are expected to be mostly oxygen atoms in the protein, the errors by using an all-oxygen standard will be small, though not necessarily negligible. A similar problem occurs when comparing the protein in solution with its crystalline form, and our more detailed analysis below finds an even larger change on crystallization, namely, a change from hexa- to tetracoordinated.

One can do better by the fitting method, where the contributions from a mixture of oxygen and nitrogen atoms can be taken into account, and we present such an analysis. We use as our standard for oxygen backscattering the compound Zn-Ntr with six oxygens surrounding the Zn atom at an average distance of 2.096 Å and a mean square variation in this average due to structural variations of $\sigma^2 = 0.0045$ Å^2 (Ferrari et al., 1967). The nitrogen standard is zinc hexaimidazole dichloride (Zn-imidazole) as a crystal (Garrett et al., 1983). The average Zn–N bond is 2.193 Å, with a negligible structural mean square variation about this average. In the fitting $\sigma^2 = 0.001$ Å^2 is added, where appropriate, to the structural variation of the protein in order to compensate for the differences in energy dependence of the XAFS signal between measurements in the transmission and fluorescence modes, as discussed under Theory, since we usually measure the standards in the transmission mode and the protein species in the fluorescent mode. To obtain the total σ^2, the thermal vibrations at room temperature must be added to these values. Since Zn-Ntr was measured only at room temperature, its thermal vibration was determined by a log ratio comparison with Ni-Sft and Ni-Fmt, both of which were measured at 80 and 300 K. The temperature dependence of the latter two standards was determined from a log ratio plot, and this dependence was fit by an Einstein oscillator model to obtain their total σ^2 at room temperature. By this means the total mean squared disorder values at room temperature for Zn-Ntr, Ni-Sft, and Ni-Fmt were determined to be 0.0090 (3), 0.0060 (3), and 0.0067 (6) Å^2, respectively. The $k^3\chi(k)$ values of these standards are shown in Figure 3.

Figure 4 is the magnitude of the Fourier transform of the room temperature $k^3\chi(k)$ of the Zn-Ca protein in solution and when crystallized. Figure 5 shows the corresponding transforms for the standards. The windows used for isolating the first shell are shown in Figures 4 and 5. They have a full-width at half-maximum of 1.10 Å with Hanning tapers on each side of total width 0.2 Å each. The window for the protein solution is centered at 1.56 Å, for the crystallized protein at 1.62 Å, for the Zn-Ntr at 1.59 Å, and for the Zn-imidazole at 1.62 Å. The uncertainties for the fitting of this protein were determined as discussed under Theory and are plotted in Figure 6.

Table II: Fitting the Zn Coordination Shell in Concanavalin A by Zn-O and Zn-N Standards[a]

atom	number	R (Å)	$\Delta\sigma^2$ (Å^2 × 10^{-4})	goodness	freedom
Fit of Zn-Ca Protein Crystal by Zn-O (Zn-Ntr) and Zn-N (Zn-imidazole)					
O	4	2.04 (2)	46 (30)	1.4	5
O	3	2.02	18	3.2	3
N	1	2.19	−71		
N	4	2.10	−42	18.0	5
O	4	2.04	47	0.7	3
N	1	2.20	403		
O	3	2.03	34	1.0	3
N	2	2.14	69		
O	2	2.01	19	0.9	3
N	3	2.14	5		
O	1	1.98	−19	1.4	3
N	4	2.13	−20		
Fit of Zn-Ca Protein Solution by Zn-O (Zn-Sft) and Zn-N (Zn-imidazole)					
O	6	2.11	50	10.1	5
O	5	2.10 (2)	17 (30)	1.6	3
N	1	2.38 (5)	−100 (90)		
O	4	2.09	−5	3.8	3
N	2	2.32	−49		
Fit of Zn-Ca Protein Solution by Zn-O (Zn-Ntr) and Zn-N (Zn-imidazole)					
O	5	2.10	20	2.0	3
N	1	2.38	−90		
O	4	2.09	1	2.4	3
N	2	2.32	−42		
Fit of Zn-Only Protein Solution by Zn-O (Zn-Ntr) and Zn-N (Zn-imidazole)					
O	5	2.09	41	3.5	5
O	4	2.07 (2)	47 (40)	0.9	3
N	1	2.22 (5)	−100 (90)		
O	3	2.05	29	1.5	3
N	2	2.21	−81		
O	2	2.03	1	3.2	3
N	3	2.20	−75		

[a] The first column is the atom type (O for oxygen and N for nitrogen). The second is the number of atoms in the first coordination shell. R is the average distance from the Zn site and $\Delta\sigma^2$ is the disorder about R relative to that of the standards. Goodness is the χ^2_ν value. Freedom is ν, the degrees of freedom remaining after the use of the fit parameters. The standards used in a particular fit are indicated in parentheses above each set of fit results. Only the acceptable fits have their uncertainties indicated in the table. The rest of the fits are unacceptable because of too large χ^2_ν or other criteria discussed in the text. The number of atoms were fixed in the fitting while R and $\Delta\sigma^2$ were adjusted. All the data were taken at room temperature.

The best fit to the data was obtained from a nonlinear fitting routine applied to eq 8. The results for various models with variations in the distribution among the N and O atoms but with fixing the total coordination to agree with the log ratio results are listed in Table II. The parameters varied in the fit were R and σ^2 for each atom type. Thus, when both N and O are used, four parameters are employed while only two are used for all of one type of ligand. In Table II are given, for each model, the best values of R_O, R_N, $\Delta\sigma^2_O$, $\Delta\sigma^2_N$, the degrees of freedom ν, and the value of χ^2_ν, where the subscripts refer to either oxygen (O) or nitrogen (N) atoms. Note that both the standards and the proteins are at room temperature and the $\Delta\sigma^2$ are the differences between standards and proteins. The evidence that standards are good ones is further confirmed by the small shifts in their E_0 required to obtain the best fit to the proteins. For the crystal these shifts are 1.0 eV for Zn-Ntr and −0.5 eV for Zn-imidazole while for the solution they are −0.3 and 0.2 eV, respectively. As noted from Table II, neither the crystallized nor the dissolved protein can be fit by all N or all O ligands. The crystal has several mixtures of nitrogen and oxygen ligands that have χ^2_ν near one. In fact, one to four nitrogen neighbors with corresponding oxygen neighbors to complete the pentacoordination are all reasonable fits as is a tetracoordination of four oxygens. All other coordinations and mixtures of N and O atoms had χ^2_ν greater than 3 and were considered not acceptable. The solution has only two reasonable fits, namely, with one or two nitrogen atoms and oxygen ligands that complete the hexacoordination. Even the best of these two fits with one nitrogen has a χ^2_ν of 2.0, which is somewhat above a good fit. However, our estimates of nontransferability uncertainties are rather crude and it is not unreasonable that we have underestimated these errors in this case by an amount to explain this value of χ^2_ν. To check this point we used as the Zn–O standard Ni-Sft instead of Zn-Ntr. To correct for the Ni center atom we used theory to calculate the difference in the phase $\delta_j(k)$ of eq 1. With this new standard a better fit was obtained with a χ^2_ν = 1.6, proving that transferability variability is of the correct order to explain the χ^2_ν values. With this new standard only the one-nitrogen case is acceptable; the two-nitrogen case has χ^2_ν = 3.8.

The fits do not define the crystal so uniquely and we have to use other criteria to distinguish between the various acceptable models. The best fit of four oxygens and one nitrogen has an unreasonably large $\Delta\sigma^2_N$ = 0.04 Å^2. The Zn-imidazole standard has about the same Zn–N distance as fitted for the protein and one would expect similar thermal disorder for the two so that the $\Delta\sigma^2_N$ should be an order of magnitude smaller than its fitted value. The unreasonably large value of $\Delta\sigma^2_N$ tends to eliminate the contribution of the one nitrogen ligand and we take the hint to conclude that the N should not be present. The other three cases of mixed oxygen and nitrogen ligands have acceptable values of $\Delta\sigma^2$ but are considered not acceptable because of the following. The most likely amino acid to donate a nitrogen ligand is a histidine, which produces prominent structure in the R-space transform around 3–4 Å. This is apparent in Figure 5 for the Zn-imidazole standard, which has six imidazole neighbors. Scaling this structure for the two to four imidazole rings associated with the corresponding number of histidine ligands, one expects a larger structure in the 3–4-Å range than is observed for the crystal in Figure 4.

Another (though related) observation in support of the absence of histidine ligands in the crystal is a characteristic structure in the $\chi(k)$ plot produced by imidazole ligands, as can be seen in Figure 3 for the Zn-imidazole standard.

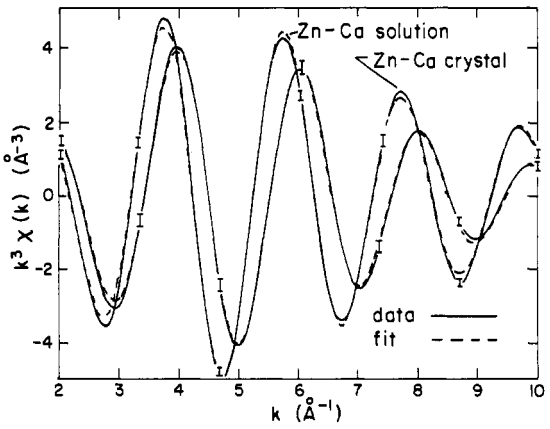

FIGURE 7: Fits (---) to the filtered $k^3\chi(k)$ spectra (—), obtained with one nitrogen and five oxygens for Zn-Ca concanavalin A solution and with four oxygens for the crystal. The uncertainties squared are σ_i^2 times ν/N_I to scale for the loss of degrees of freedom with the use of fit parameters.

Whereas the non-imidazole-containing standards show a single peak at the oscillation peaking at 4 Å^{-1}, the imidazole standard shows a splitting into two peaks. This behavior is a common feature of imidazole ligands as published in the literature (Co et al., 1981; Strange et al., 1986). It is understood as an interference of the contribution from the prominent structure in the 3–4-Å region. We note in Figure 2 that both the Zn-Ca solution and the Zn-only solution have a hint of this splitting appropriate for one histidine instead of the six in the standard. However, the Zn-Ca crystal shows no hint of this splitting, consistent with the conclusion that there are no histidine as ligands. We therefore eliminate the cases with N ligands as acceptable models and remain with the preferred fit of four oxygen ligands.

The tetracoordinated structure is a quite drastic change from the solution structure and it is comforting to obtain more confirming evidence for its validity. Such confirming evidence is obtained from the near edge spectrum of ZnO which is a tetracoordinated structure of Zn. Its near-edge spectrum is plotted in Figure 1 and it is noted that it has a smaller peak, similar to the one in the crystallized Zn-Ca concanavalin A. The shape of the peak is different with sharper features but they are explained by contributions from the second and further neighbor atoms, which give more prominent contributions in this compound compared to the other samples. The important feature is that this four-coordinated compound has a significantly smaller peak than six-coordinated samples and the area of its peak is similar to that of the protein in the crystal.

Figure 7 shows the acceptable fits in k-space compared to the data for the isolated first shell for (a) the solution and (b) the crystal. The acceptable fit for the crystal is four oxygen ligands at 2.040 ± 0.02 Å with a σ^2_O = 0.014 ± 0.003 Å^2. The acceptable fit for the solution is five oxygen ligands at 2.10 ± 0.02 Å with σ^2_O = 0.008 ± 0.003 Å^2 and one nitrogen at 2.38 ± 0.05 Å with $\Delta\sigma^2_N$ = −0.010 ± 0.009 Å^2. Note that we give absolute values of σ^2 for the oxygen atoms while only differences for the nitrogen because we obtained the absolute σ^2 values for only the oxygen standards. Although the $\Delta\sigma^2_N$ for this latter case is somewhat large, it is negative and four times smaller than the case we reject for the Zn-Ca crystal, and, with its uncertainty, it is consistent with the values of the Zn-imidazole standard. The values of σ^2_O include both structural and vibrational contributions while the $\Delta\sigma^2_N$ has only a vibrational contribution. Since there are four or five oxygens that contribute to the σ^2 of the first coordination shell, variation

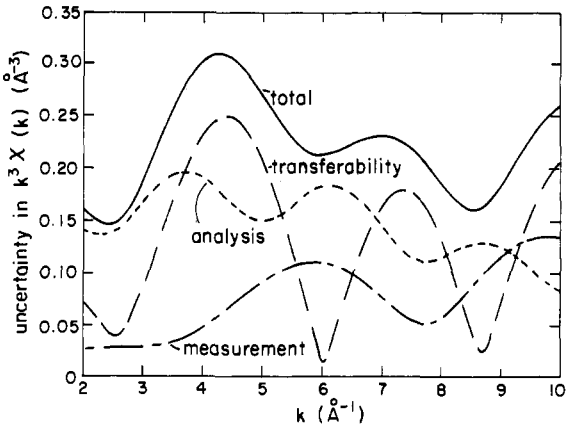

FIGURE 8: Uncertainties for fitting Zn-only concanavalin A solution.

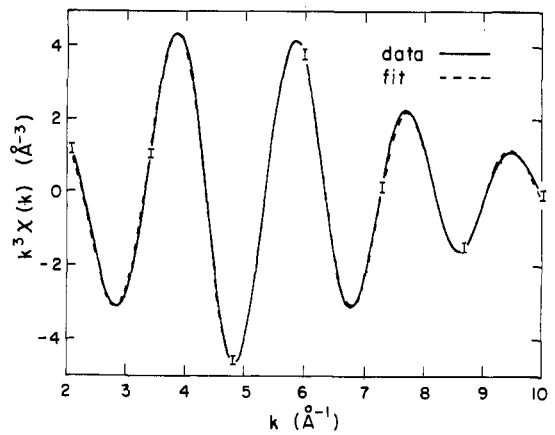

FIGURE 9: Fit (---) to the filtered $k^3\chi(k)$ spectrum of Zn-only concanavalin A solution (—), obtained with one nitrogen and four oxygens. The uncertainties squared are σ_i^2 times ν/N_I to scale for the loss of degrees of freedom because of the fit parameters.

in the ligand bond distances caused by the different residues that are bound are expected to add the additional structural contribution and to give a larger σ^2 than found for the single nitrogen ligand. The values we find are well within a reasonable range.

(*b*) *Beyond the First Shell.* Differences between the crystal and solution are also seen outside the coordination shell of the Zn atom. Figure 4 shows the Fourier transforms of the XAFS in *R*-space. Beyond $R \approx 4.5$ Å, the data are dominated by noise and are out of the sensitivity of the experiments. Within this distance, differences occur everywhere. Beyond the first shell the Fourier transforms in the region from 2 to 4.5 Å show that the crystal has a much lower magnitude of the transform than the solution. One cause for this is the presence of an imidazole ring in the solution with its prominent structure between 3 and 4 Å that is absent in the crystal.

We demonstrate that the changes include phase differences in the XAFS by performing an inverse Fourier transfer to *k*-space with an *R*-space-filtering window from 3.1 to 4.1 Å. In comparing the magnitude of the inverse Fourier transforms of the crystal and solution as well as their *R*-space differences, we find that the amplitude of the latter is nearly equal to the difference in the amplitudes of the crystal and solution from $k = 2$ to 4 Å^{-1}, an indication that their signals are in phase in this region. From $k = 6$ to 8 Å^{-1}, the amplitude of the transformed difference is greater than those to both the crystal and solution, indicating that they are out of phase in this range. At even higher *k* values, noise is dominant and the phases look random. The *k*-dependence described above indicates that there is a distribution change in atoms from solution to crystal beyond the first coordination shell, which cannot be described merely by a Debye–Waller factor.

Although these changes beyond the first shell cannot be discussed more quantitatively, they give additional confirmation of our notion that the alteration in the Zn coordination shell is a part of a more extensive conformational change of the protein molecule (Lin et al., 1990).

(*c*) *Effects of Cryoprotectant.* In the temperature dependence study, MPD or galactose was added to the protein crystal or solution, respectively, to prevent ice crystal formation. At room temperature these samples are compared with those without the cryoprotectants by the log ratio method. The results are listed in Table I.

The effect of galactose on the Zn site in solution is chiefly an increase of its disorder by ~0.002 Å^2. In the solution preparation we added 40% (by weight) of galactose in the sample, which constitutes a molar ratio of galactose to protein on the order of 1000:1. The high concentration of galactose may change the hydration shell around the protein molecules. Galactose does not bind to concanavalin A (unpublished data), and we need not consider specific galactose–protein interactions as a major contribution to the disorder increase. The main point is that the coordination around the Zn in the solution is not modified by the galactose. For the crystal the cryoprotectant MPD has no detectable effect at the Zn site.

Both results indicate that the addition of cryoprotectants to the protein samples would not influence our comparison of the protein crystal and its solution. Our conclusions about the coordination number change on crystallization, and the abnormal thermal behavior of the crystal, have nothing to do with the cryoprotectants.

(*d*) *Effects of Removing the Second Metal.* A concanavalin A sample with the Ca removed from the site S2 was measured in solution at room temperature. Previously, the crystal of such a sample had been measured by XAFS (Kalb et al., 1979) and it was determined to be hexacoordinated. To the best of our knowledge an S1-occupied and S2-empty concanavalin A crystal structure has not been published. The $k^3\chi(k)$ for this sample is plotted in Figure 2. The results of a log ratio comparison with the crystal and solution of Zn-Ca are listed in Table I. For comparison, the previous crystal results (Kalb et al., 1979) are also listed. Focusing on the comparisons of solution and crystal with the common Zn-Ca crystal, we note that within uncertainties both forms of the protein without Ca are the same. In contrast with the protein containing Ca, no change on crystallization appears to occur. However, the solution with and without Ca does change coordination by one; a ligand is lost when the Ca is removed. Thus our latest results are that the crystal without Ca is pentacoordinated, not hexacoordinated as suggested previously (Kalb et al., 1979). A fitting routine was performed on the first coordination shell of the Zn atom of the solution with the same standards and method as for the Zn-Ca case. The uncertainties in this case are shown in Figure 8. The results of the fit are shown in Table II. In this case only two models give satisfactory fits, namely, one or two nitrogens with the rest of the ligands being oxygen to complete the pentacoordination. The case of four oxygens and one nitrogen is chosen as the preferred model because of the absence of prominent structure in the 3–4-Å range in Figure 4 for the Zn-only protein. The fit to the isolated first shell data is shown in Figure 9 for the case of one nitrogen.

As an aside, our previous result (Kalb et al., 1979) was in error because we used as a standard ZnO. This standard has a problem that was not appreciated at the time. It has a second shell from the Zn–Zn scattering that is much larger than the first Zn–O shell. When the first shell is "isolated", significant leakage from the second shell is included to produce the error.

Discussion and Conclusions

The XAFS measurements on the S1 site of concanavalin A when occupied by Zn show dramatic changes in its structure between the dissolved and crystallized states. When the S2 site is occupied by Ca the solution is hexacoordinated at the S1 site and tetracoordinated when crystallized. In contrast, when the S2 site is unoccupied, the S1 site is pentacoordinated in both the solution and the crystal and no significant change occurs on crystallization. According to our analysis, an oxygen atom is released on going from hexa- to pentacoordination and a nitrogen atom leaves on going from penta- to tetracoordination.

The importance of ascertaining structural differences of a protein between a crystal and a solution is illustrated by the Zn concanavalin A protein we have investigated. When the S2 site has its Ca atom removed the saccharide-binding site is destroyed, presumably due to a modified conformation. If the crystal structures were used to ascertain these conformational changes, they would be in error, since we find that the coordination number changes are opposite in the crystal and in the solution. Any conclusions drawn from *crystal* structure determinations could lead to an erroneous mechanism for the change in the protein's property in *solution*.

Crystal structure determinations on concanavalin A with the S2 site filled by Ca and the S1 site filled with Mn or unspecified metal atoms (Hardman & Ainsworth, 1972; Edelman et al., 1972; Becker et al., 1975; Hardman et al., 1982) indicate a hexacoordinated S1 site, in contrast to the tetracoordinated one we have determined for Zn on this study. This suggests that the coordination at the S1 site depends on the atom occupying that site. We have measured the coordination at the S1 site when it is occupied by other transition metals and do find a change in coordination, which will be reported in a separate publication. The crystal structure for Mn-Ca crystals indicates that when it is hexacoordinated, the metal atom is liganded to two water oxygens, one histidine nitrogen, and three carboxylic oxygens. Our results on the hexacoordinated Zn-Ca solution are consistent with this result since we find five oxygen and one nitrogen ligands. The loss of an oxygen ligand can be easily accepted by assuming it is an exchangable water molecule [cf. Meirovitch and Kalb (1973)], but the loss of the nitrogen indicates that a histidine residue is released, which must cause a substantial conformational change, in agreement with our results. The conformational changes are not limited to the first neighboring shell around the Zn. Up to the detection limit of XAFS of 4.5 Å, changes are observed when the protein crystallizes. In addition, removing the Ca at the S2 site, which is about 4.5 Å from the Zn, produces conformational changes at the S1 site, giving additional evidence of long-range conformational changes. The changes on crystallization are all the more dramatic when it is noted that the S1 site is about 10 Å from the surface of the protein as determined by crystal diffraction measurements.

Our results show that the Zn atom in concanavalin A is capable of adopting at least three different configurations, characterized by a four-, five-, or six-membered ligand shell. We find different bond distances are associated with each of the different coordinations, the average distance being 2.04, 2.09, and 2.15 Å as the coordination increases from four to five to six, respectively.

Zinc has a propensity to have these three coordination numbers, and the changes in average bond distances are comparable with the values found for such structures. For example, ZnO, bis(acetylacetone)zinc monohydrate, and ZnNtr have, respectively, four, five, and six oxygen atoms coordinated to the Zn and their average bond distances increase by 0.03 Å and 0.076 Å as the coordination numbers increase from four to five and from five to six, respectively (Wyckoff, 1965).

The crystals used in the XAFS measurements were grown in the same way as those used for X-ray diffraction measurements from solutions similar to the ones used in the XAFS measurements. We made careful tests on the effects of possible spurious effects that could cause changes from the dissolved and crystallized protein such as the added cryoprotectants and pH differences and found no such effects.

The analyses described here were able to distinguish between oxygen and nitrogen neighbors. It is sometimes claimed that XAFS cannot make such a distinction. We succeeded in making this distinction for two main reasons. One, the standards we used were quite good. But more importantly, we used a criterion that gives an objective measure of when a satisfactory fit occurs, namely, the normalized χ^2_ν function of eq 8. The success of this method requires an accurate assessment of experimental uncertainty. Besides measurement uncertainties, the uncertainties in analyses and in lack of transferability between standards and the proteins need to be taken into account. In fact, these latter two uncertainties dominated!

The results reported here suggest an explanation for the interesting observation that the degree of disorder in concanavalin A crystals depends on the identity of the atom in the S1 site [Kalb (Gilboa) et al., 1988]. If one assumes that the susceptibility of the S1 site to conformational change under the action of the intermolecular forces of crystallization depends on the cation occupying the site, the crystal disorder results can be understood. Those with more disorder have more variations under crystallization interactions. Measurements are planned to determine directly from XAFS the variation of the susceptibility of the S1 site to change under crystallization to ascertain whether this correlates with the observed disorder.

Because a single technique was used to measure the structure in solution and crystal, high sensitivity to changes about the metal site when the protein crystallizes is possible. In the case of concanavalin A with Zn in the S1 site, the changes about the zinc are quite dramatic and easily detected, but much more subtle changes can be detected by XAFS. The changes about the Zn site are particularly dramatic when it is noted that the site is ~10 Å from the protein surface as determined by crystal structures. When a protein crystallizes, intermolecular contacts occur along portions of the surface. As shown previously (Lin et al., 1990), such intermolecular interactions introduce stresses in the protein and, at least in one of the cases studied here, changes the conformation of the protein even far from the surface. The significance of this result depends on how generally proteins have their conformations modified on crystallization. However, the results presented here indicate that some caution is in order in assuming, as a general rule, that crystallization does not significantly perturb protein conformations.

Acknowledgments

Research was supported by NSF Grant DMB-8613948. We are grateful for the assistance of L. Fareria, J. Scrofani, and Dr. G. Lamble on beam line X11A of NSLS. Beam line X11A is supported by DOE Contract DE-AS05-80-ER 10742. The NSLS facility is supported under DOE Contract DE-AC0276CH00016.

Registry No. ZnO, 1314-13-2; Ni-Sft, 66634-47-7; Ni-Fmt, 15694-70-9; Zn-Ntr, 10196-18-6.

References

Becker, J. W., Reeke, B. N., Jr., Wang, J. L., Cunningham, R. A., & Edelman, G. M. (1975) *J. Biol. Chem. 250*, 1513–1524.

Braun, W., Wider, G., Lee, K. H., & Wüthrich, K. (1983) *J. Mol. Biol. 169*, 921–948.

Brewer, C. F., Sternlicht, H., Marcus, D. M., & Grollman, A. P. (1973) *Biochemistry 12*, 4448–4457.

Clore, G. M., et al. (1987) *Protein Eng. 1*, 313–318.

Co, M. S., Scott, R. A., & Hodgson, K. O. (1981) *J. Am. Chem. Soc. 103*, 986–988.

Derewenda, Z., Yariv, J., Helliwell, J. R., Kalb (Gilboa), A. J., Dodson, E. J., Papiz, M. Z., Wan, T., & Campbell, J. (1989) *EMBO J. 8*, 2189–2193.

Ferrari, A., Braibanti, A., Manotti Lanfredi, A. M., & Tiripicchio, A. (1967) *Acta Crystallogr. 22*, 240–246.

Garrett, T. P. J., Guss, J. M., & Freeman, H. C. (1983) *Acta Crystallogr. C39*, 1027–1031.

Goldstein, I. J., & Hayes, C. E. (1978) *Adv. Carbohydr. Chem. Biochem. 35*, 127–340.

Hardman, K. D., Agarwal, R. C., & Freiser, M. J. (1982) *J. Mol. Biol. 157*, 69–86.

Johansen, J. T., & Vallee, B. L. (1975) *Proc. Natl. Acad. Sci. U.S.A. 69*, 2850.

Kalb, A. J., & Levitzki, A. (1968) *Biochem. J. 109*, 669–672.

Kalb (Gilboa), A. J., Stern, E. A., & Heald, S. M. (1979) *J. Mol. Biol. 135*, 501–506.

Kalb (Gilboa), A. J., Yariv, J., Helliwell, J. R., & Papiz, M. Z. (1988) *J. Crystal Growth 88*, 537–540.

Kline, A. D., et al. (1986) *J. Mol. Biol. 189*, 377–382.

Lee, P. A., Citrin, P. H., Eisenberger, P., & Kincaid, B. M. (1981) *Rev. Mod. Phys. 53*, 769–806.

Lin, S. L., Stern, E. A., Kalb (Gilboa), A. J., & Zhang, Y. (1990) *Biochemistry 29*, 3599–3603.

Lu, K.-Q., & Stern, E. A. (1983) *Nucl. Instrum. Methods 212*, 475–478.

McMaster, W. H., Kerr Del Grande, N., Mallett, J. H., & Hubbel, J. H. (1969) *Compilation of X-ray cross sections*, National Technical Information Service, Springfield, VA.

Meirovitch, E., & Kalb, A. J. (1973) *Biochim. Biophys. Acta 303*, 258–263.

Pflugrath, J. W., et al. (1986) *J. Mol. Biol. 189*, 383–386.

Quiocho, F. A., & Lipscomb, W. N. (1971) *Advances in Protein Chemistry* (Edsall, J. T., Anfinsen, C. B., & Richards, F. M., Eds.) Vol. 25, pp 1–78, Academic Press, New York.

Reeke, G. N., Hartsuck, J. A., Ludwig, M. L., Quiocho, F. A., Statz, T. A., & Lipscomb, W. N. (1967) *Proc. Natl. Acad. Sci. U.S.A. 58*, 2220–2226.

Sage, J. T., Morikis, D., & Champion, P. M. (1989) *J. Chem. Phys. 90*, 3015–3032.

Schultze, P., Wörgötter, E., Braun, W., Wagner, G., Vaâk, M., Kägi, J. H. R., & Wüthrich, K. (1988) *J. Mol. Biol. 203*, 251–268.

Shoham, M., Kalb, A. J., & Pecht, I. (1973) *Biochemistry 12*, 1914–1917.

Stern, E. A., & Heald, S. M. (1983) *Handbook on Synchrotron Radiation* (Koch, E. E., Ed.) Vol. 1, pp 955–1014, North-Holland Publishing Company, Amsterdam.

Strange, R. W., Hasnain, S. S., Blackburn, N. J., & Knowles, P. F. (1986) *J. Phys., Colloq. 47*, C8, 593–596.

Sumner, J. B., & Howell, S. F. (1936) *J. Bacteriol. 32*, 227–237.

Von Krogmann, K., & Mattes, R. (1963) *Kristallographie*, 291–302.

Wagner, G., et al. (1987) *J. Mol. Biol. 196*, 611–638.

Wüthrich, K. (1989) *Acc. Chem. Res. 22*, 36–44, and references cited therein.

Wyckoff, W. G. (1965) *Crystal Structures*, 2nd ed., Wiley, New York.

Yariv, J., Kalb, A. J., & Levitzki, A. (1968) *Biochim. Biophys. Acta 165*, 303–305.